Cascade Fluorescence Modulation in Photochromic Microcapsules

Magin Benedict Ferrer, Daiyu Harada, Colin Martin, Rémi Métivier, Clemence Allain, Keitaro Nakatani, Marine Louis, Noriaki Kawaguchi, Takayuki Yanagida, Kazuma Yasuhara, et al.

ACS APPLIED MATERIALS & INTERFACES

www.acsami.org
Research Article

Cascade Fluorescence Modulation in Photochromic Microcapsules

Magin Benedict Ferrer,[#] Daiyu Harada,[#] Colin J. Martin, Rémi Métivier, Clémence Allain, Keitaro Nakatani, Marine Louis, Noriaki Kawaguchi, Takayuki Yanagida, Kazuma Yasuhara,* and Tsuyoshi Kawai*

Cite This: ACS Appl. Mater. Interfaces 2024, 16, 57626−57635
Read Online

ACCESS | Metrics & More | Article Recommendations | Supporting Information

ABSTRACT: Certain derivatives of terarylene are able to undergo a highly efficient oxidative cycloreversion cascade effect, a ring opening reaction with quantum yields above unity, resulting in a colored-to-colorless transition in solution. In the presence of chloroform, high-energy UV and X-rays can trigger this phenomenon, potentially acting as a visual detection system for ionizing radiation. However, chloroform is sensitive to different irradiation wavelengths without distinction, making it difficult to adapt to a reusable device. Chlorobenzene was chosen as an alternative halogenated solvent, as it offers wavelength selectivity between photocyclization and cascade effect cycloreversion. Nile Red was also incorporated into the system with the aim of improving the sensitivity of the visual detection via fluorescence photoswitching. Finally, microencapsulation of both terarylene and Nile Red was targeted to obtain both the cascade effect and photoswitching in a single system. In microcapsules made from a Pickering emulsion, this terarylene−Nile Red system showed high fatigue resistance to repeated photocyclization and cycloreversion irradiation, giving access to repeated ON/OFF fluorescence photoswitching. The cascade effect was also successfully demonstrated along with fluorescence recovery, showing the versatility of the two phenomena in different media.

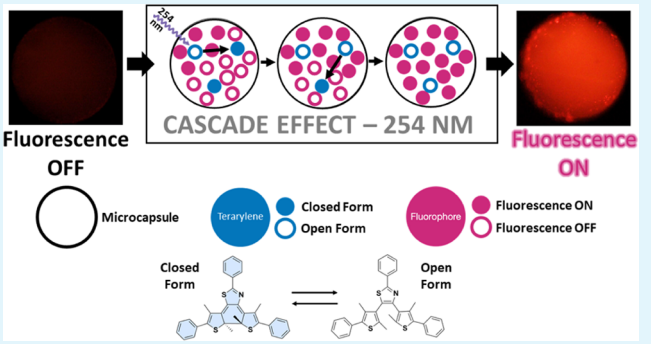

KEYWORDS: *cascade effect, photochromism, fluorescence, oxidative cycloreversion, Pickering emulsion*

1. INTRODUCTION

Traditional photomultiplier tubes,[1] solid-state photomultipliers,[2−4] and avalanche photodiodes[5,6] work by exploiting the cascade effect in which a weak signal such as a single photon can produce effects involving a large number of molecules. Pure organic-based detectors operating under the same principle have been developed where the output response is observed as a color change.[7] Organic detectors have also been explored based on the photochemical electrocyclic reaction of diarylethene (DAE) derivatives.[8−10] Recently, these systems have been further expanded using terarylenes (TA).[11,12] Their absorbance and electrochemical properties[12−14] have been widely modified by using thiazole groups,[15] extending the π-conjugation system,[16−18] or adding different functional groups.[19,20]

This cascade effect was first observed in 1995 for a DAE derivative using cyclic voltammetry in acetonitrile to bring about oxidative cycloreversion that implied at least six ring openings from a single oxidation source.[21] Similar phenomena have also been reported in modified DAEs.[17,19,22−24] This phenomenon was later demonstrated for several TA derivatives, which typically display 1000 ring opening reactions after a single chemical oxidation by tris(*p*-bromophenyl)ammonium hexachloroantimonate ($TBPA^{\bullet+}$).[12] The oxidation trigger was further achieved with UV light irradiation in chloroform, and the apparent photochemical quantum yield reached 33 (3300%).[25] This reaction involves photochemical charge transfer−photoexcitation between TA and chloroform with quantum yields much higher than the typical values for cycloreversion upon visible light irradiation of the same family of compounds, mostly less than 0.08.[11,15] In general, this cascade effect occurs starting from the closed form (CF) isomer in solution. In the presence of an oxidizing trigger, the radical cation $CF^{\bullet+}$ is generated followed by a spontaneous ring opening to the radical cation of the open form ($OF^{\bullet+}$). This is followed by an exothermic charge transfer with another CF molecule, generating an additional $CF^{\bullet+}$ and continuing the chain reaction mechanism (Scheme 1).

Received: June 5, 2024
Revised: September 14, 2024
Accepted: September 17, 2024
Published: September 25, 2024

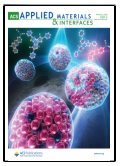

Scheme 1. Illustration of the Cascade Effect System in Bulk Solution (Previous Reports) vs in a Microcapsule System (This Work)

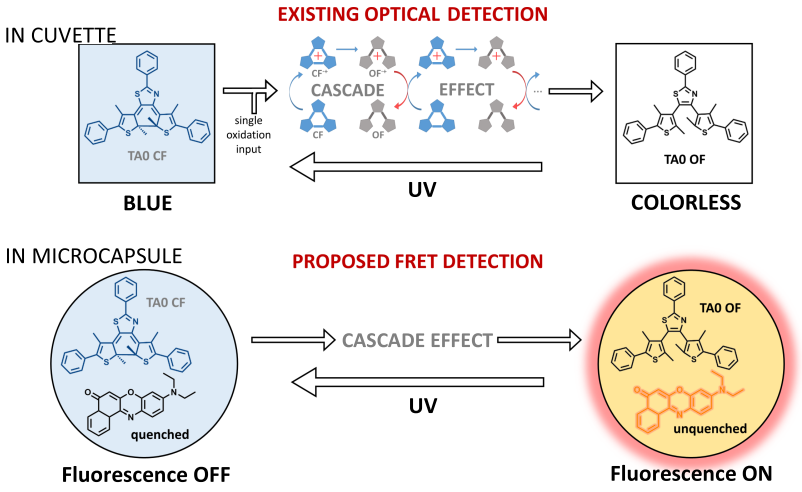

Radiation detection is important in assessing the safety of the environment and individuals subjected to occupational exposure in hospitals or in nuclear power plants.[26] To avoid exposure at high doses in these environments, personal dosimeters have been developed that measure individual doses either passively, where measurements are done after use, or actively, where readouts are provided in real time.[27−32] Active dosimeters have also been developed based on organic color changing where ionizing radiation can cause polymerization or isomerization between two forms of different colors.[33−37] Nonetheless, the risks of long-term exposure at low doses remain uncertain.[26]

Recently, some of us investigated other TA derivatives containing a thiazolyl bridging unit and phenyl thiophene side arms and showed that the cycloreversion cascade effect could be induced by UV or X-ray initiation.[25] This was achieved by using a halogenated solvent mixture of 9:1 chloroform:toluene. Under the ionizing irradiation of UV−B or X-rays, halogenated solvents such as chloroform facilitate the formation of the radical $CF^{\bullet+}$.[25] This system will remain usable as long as appropriate measures are taken to ensure the absence of chloroform during the initial photocyclization of the OF to the CF and the subsequent photocyclizations after each cascade effect event. The cascade effect was reported to be highly sensitive to X-rays, with doses as low as 0.3 mGy, whereas other previous organic molecules have only reached sensitivities as low as 50 mGy.[37] This makes TA derivatives exhibiting the cascade effect in solution an excellent target for further developments.

However, there are still challenges yet to be conquered in the journey toward developing cutting-edge dose-sensing materials based on this system.[38,39] As the ionizing radiation needs to be mediated through photo-oxidizing chemistry, chloroform has been used as a solvent. However, this proved to be sensitive to both UVA and UVB without distinction, reducing the ring closing efficiency of TA with UVA and enhancing the difficulty of repetitive CEs. Besides, in previous reports, the cascade amplification was detected only via the change in color measured through the visible light absorption of the photochromic molecule.[11,12,25] Although Yamaguchi and Irie demonstrated promising radiosensitivity of DAE derivatives via turn-on fluorescence detection, achieving the same for CE systems remains challenging.[37] This motivated us to avoid complicated molecular design and to focus instead on multicomponent systems for fluorescence mode radiation detection. Another issue to be tackled is that these CE systems require solution-phase intermolecular electron exchange reactions. This presents an intrinsic difficulty, making them challenging to handle in either solid or polymer films. Furthermore, the CE capability strongly depends on solution mixing, which usually requires mechanical stirring or ultrasonication. In the present work, the possibility of microscale dosimeters was explored via the fabrication of biopolymeric microcapsules (Scheme 1), which offer the possible advantage of small-scale embedding of the liquid system in solid matrices.[40,41] As the characteristic diffusion length of most chemical substances is on the order of several tens of μm, mixing conditions become less critical for microcapsules smaller than 100 μm in diameter. We here assessed several halogenated solvents to replace chloroform and screened their wavelength selectivity during both CE fading and normal coloration of the TA derivatives. Concurrently, a further increase in sensitivity to enable visual detection was targeted through pairing of the derivative **TA0** (Scheme 1), showing efficient CE fading, with a fluorophore, to observe fluorescence change. Based on the Förster resonance energy transfer (FRET) between the fluorophore and **TA0** in the CF,[42,43] we here explore fluorescence-based UV sensing in the UVC range (254 nm) that accompanies CE activity. This is expected to be more sensitive in comparison to the existing optical detection methods based on color changes in solution.

2. MATERIALS AND METHODS

Unless otherwise noted, reagents and solvents were purchased from commercial suppliers and used without further purification. Solvents used for analysis were spectroscopic grade. Column chromatography was carried out using silica gel with chloroform as the eluent. 99% (metal basis) calcium carbonate nanopowder (CA-CB-02M-NP.200NS) was purchased from American Elements.

2.1. Synthesis of 4,5-Bis(2,4-dimethyl-5-phenylthiophen-3-yl)-2-phenylthiazole (TA0). **TA0** was synthesized based on previous reports,[15] which are elaborated in the Supporting Information under the subsection with the same name.

2.2. Selection of the Halogenated Solvent. Cuvettes containing **TA0** (40 μM) in toluene were irradiated (SLUV-4 Handy UV lamp, AS-ONE) at 365 nm for 3 min to induce ring closing. The halogenated solvent was then added to the toluene

https://doi.org/10.1021/acsami.4c09023
ACS Appl. Mater. Interfaces 2024, 16, 57626−57635

solution (1:1 v/v), and the system was irradiated at 313 nm using a QYM-01 Photoreaction Quantum Yield Evaluation System, Shimadzu, or at 254 nm using the same SLUV-4 lamp to trigger the cascade effect. The absorbance of the system was followed over time at 610 nm using the same QYM-01 system. 3-point averaging was done when necessary to reduce the noise in some data.

2.3. Fatigue Resistance Experiments. Irradiation was performed using a Lightningcure 200 W Hg−Xe lamp LC8 (Hamamatsu) with the appropriate interferential filters (Semrock). A xenon lamp (75 W) was placed at an angle of 90° with respect to the irradiation beam and served as a probe light. Absorption spectra were recorded every second with a CCD instrument coupled with a spectrometer (FERGIE, Princeton Instruments). The solution was maintained at 20 °C. A toluene solution of **TA0** (40 μM, 2.5 mL) was irradiated at 365 nm up to 80% conversion compared to the photostationary state (PSS). Then, the halogenated solvent was added to the toluene solution (1:1 v/v) before further irradiation at 254 nm for 60 s to trigger the cascade effect. The 265/254 nm irradiation cycle was then repeated.

2.4. Fabrication of Microcapsules. A previously reported procedure was adapted for fabricating the oil-core microcapsules (see the SI, Workflow of Microencapsulation, Figure S1).[44]

2.5. Fluorescence Microscope Experiments. Samples were prepared by depositing microcapsules in a 10% w/w aqueous solution of PVA and then sandwiching a few drops between two glass slides. The edges of the glass slides were sealed with 10% (w/w) poly(methyl methacrylate) (PMMA) in toluene solution to avoid leakage of the microcapsules. Both absorption and emission spectra were measured using an IX71 Olympus inverted fluoresce microscope. The spectrophotometer was a USB4000 (Ocean Photonics), and the digital CMOS camera was a TC11440-36U (Hamamatsu).

3. RESULTS AND DISCUSSION

3.1. Experiments in Solution. *3.1.1. Comparative Study of the Cascade Effect Using Different Halogenated Solvents.* **TA0** belongs to a family of derivatives in which the OF exhibits absorption in the UV range (typically around 300 nm). During photocyclization, two absorption maxima are formed, one at 400 nm and another in the visible range at 610 nm, which are characteristic for the CF's extended π-electron system (Figure 1a).[9] In our previous study, photochemical coloration of the OF **TA0** was carried out under UV light (365 nm) irradiation in toluene to maximize the CF conversion ratio at the photostationary state (PSS). Chloroform was then added in a second step to trigger CE fading with UV rays or X-rays, where the oxidizing triggers generate radicals to promote highly efficient cycloreversion. To reuse **TA0** for further cycles, all the solvent needs to be removed before redissolution in pure toluene and repeating the process.[25] In fact, if chloroform is not removed before irradiation in the UV, then, simultaneous cycloreversion hinders the OF-to-CF change. Therefore, the use of a halogenated solvent that is more wavelength-selective appears necessary to gain control over both the photocyclization and cascade effect cycloreversion processes.

Both alkyl and aryl halides were chosen with different chain lengths for the former. Hence, dichloromethane (DCM), 1-chlorobutane (1-ClBut), 1-bromopropane (1-BrProp), and tetrachloroethane (TeClEt) were selected as the alkyl halide solvents, while chlorobenzene (ClBenz), bromobenzene (BrBenz), and *o*-dichlorobenzene (o-DiClBenz) were selected as the aryl halide solvents to screen viable substitutes for chloroform (Figure 1b). As for the ratio of these solvents to toluene, there must be a sufficient amount of the halogenated solvent to induce the cascade without increasing the density too much so as not to hinder microcapsule formation. DCM was chosen to test the ideal halogenated solvent-to-toluene ratio due to its similar structure to that of chloroform. A ratio of 1:1 was determined to be sufficient to induce an efficient cascade (see the SI, Figure S2), and thus, this ratio was used for all other halogenated solvents.

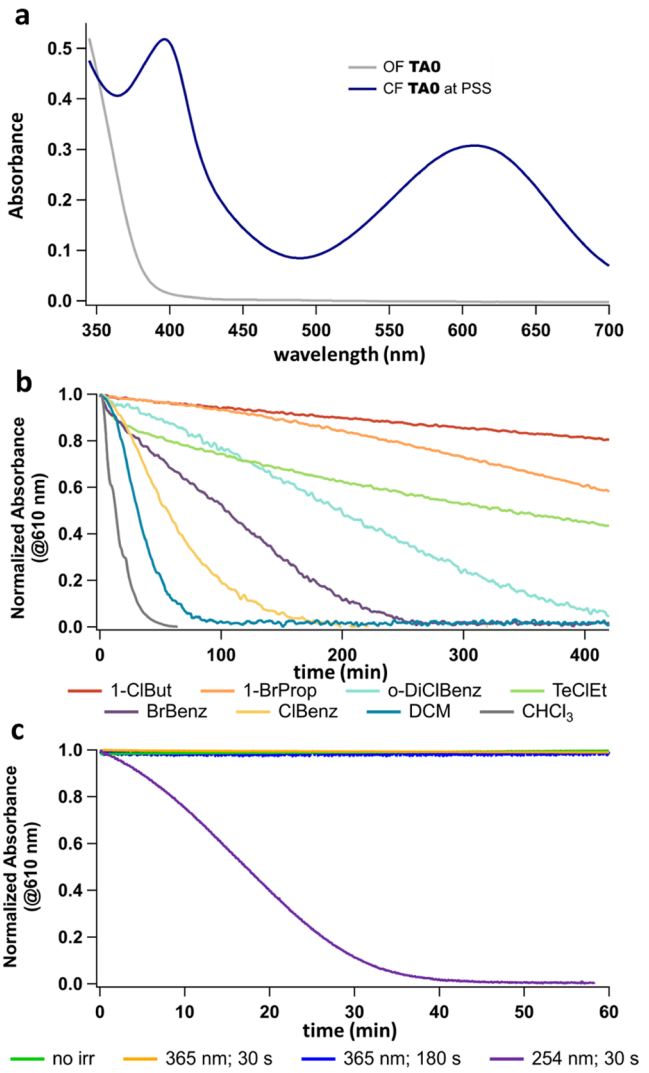

Figure 1. (a) Absorption spectra of **TA0** in toluene in its OF (gray line) and PSS (purple line). (b) Absorption time profiles of **TA0** at 610 nm (related to the CF in PSS) in halogenated solvent:toluene (1:1, v/v) after 313 nm irradiation for 30 s; [**TA0**] = 20 μM. (c) Evolution of CF **TA0** absorption (λ = 610 nm) in 1:1 ClBenz:toluene after different irradiation conditions.

TA0 was first dissolved in toluene and irradiated at 365 nm for 3 min to induce ring closure. The halogenated solvent was then added, and under stirring, the solution was irradiated at 313 nm for 30 s to trigger the cascade, and the CF absorption decay was followed by measuring the absorbance at 610 nm. Although the chloroform system showed the fastest cascade effect cycloreversion (half-life: 13 min), it was still slightly slower than in the 9:1 chloroform:toluene system previously reported (half-life: 11 min).[25] In addition to chloroform, only solutions with DCM, ClBenz, and BrBenz were able to convert **TA0** from CF to OF in a relatively short amount of time (half-lives: 31, 56, and 103 min, respectively). ClBenz was chosen as the best possible solvent due to its lower density than chloroform, which aids in the fabrication of stable microcapsules.

https://doi.org/10.1021/acsami.4c09023
ACS Appl. Mater. Interfaces 2024, 16, 57626−57635

3.1.2. Wavelength Dependence of the Cascade Effect in ClBenz:Toluene. The absorption spectra of the CF **TA0** at the PSS in the new solvent mixture (1:1 ClBenz:toluene) is similar to that in pure toluene with no observable shift in the absorption bands (see the SI, Figure S3). However, the half-life of thermal cycloreversion (3.2 days) is much faster than in toluene (14 days).[15] This has been attributed to the lower activation energy of the cycloreversion process due to the higher dielectric constant of ClBenz (ε_{ClBenz} = 5.62; $\varepsilon_{toluene}$ = 2.38), facilitating the transition from the CF to the OF as the molecule passes through various electron density rearrangements.[45,46]

To study the influence of ClBenz, the formation and evolution of the CF **TA0** in a 1:1 ClBenz:toluene mixture were measured using different irradiation wavelengths (Figure 1c): 365 nm for photocyclization and 254 nm as the cascade effect irradiation trigger.[47] First, the irradiation of OF **TA0** at 365 nm (3.0 mW) enabled the successful generation of the **TA0** PSS containing the CF without any observable competing cycloreversion behavior. Further irradiation at 365 nm showed no absorbance change. On the other hand, irradiation at 254 nm for 30 s triggered a fast decrease of the CF's characteristic absorption band (half-life: 17 min). Thus, in the ClBenz:toluene system, the ring closing and cascade-ring opening reactions can be selectively triggered by 365 nm irradiation and 254 nm irradiation, respectively. To trigger the CE process, UV light is required to promote the photoinduced redox reaction.[48] This proceeds via charge-transfer (CT) excitation between the donor and acceptor, which is dependent on both the energy difference and the dielectric constant of the medium.[25] We thus predicted that UV light at 254 nm would match the specific CT excitation band between ClBenz and CF **TA0** in the mixed solution.

3.1.3. System Reversibility. The ability of the ClBenz:toluene system to undergo repeated ring closing and CE fading cycles without degradation was also evaluated and compared with that of the chloroform system (Figures 2 and 3). When exposed to alternating irradiations at 365 nm (ring closing) and 254 nm (CE fading), the chloroform:toluene system proved unusable after four cycles due to a noticeable decrease in the amount of CF **TA0** generated after irradiation at 365 nm

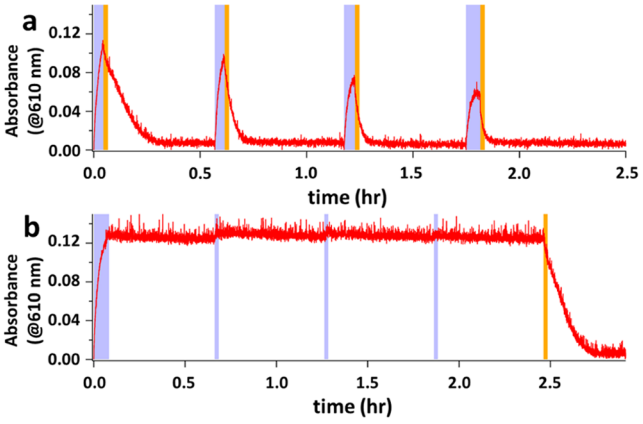

Figure 2. TA0 in 1:1 chloroform:toluene solution under repeated irradiation sequences. (a) Alternating irradiations at 365 nm(purple area) and 254 nm for 60 s (orange area). (b) Repeated irradiations at 365 nm. Subsequent 365 nm irradiations were performed with the aim of reaching the same initial absorbance. Subsequent 365 nm irradiations were performed for 60 s each.

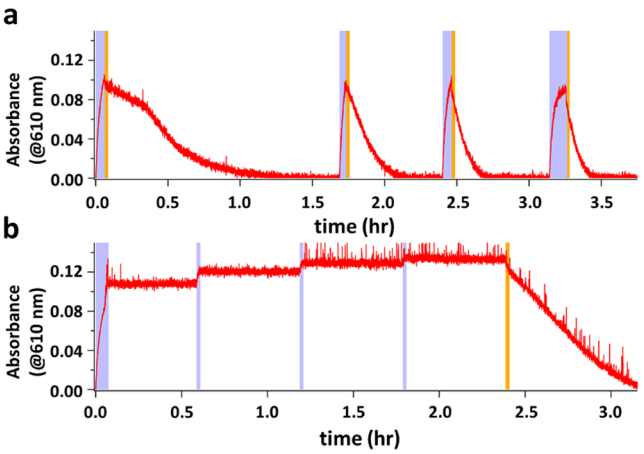

Figure 3. TA0 in 1:1 ClBenz:toluene solution under repeated irradiation sequences. (a) Alternating irradiations at 365 nm (purple area) and 254 nm for 60 s (orange area). (b) Repeated irradiations at 365 nm. Subsequent 365 nm irradiations were done with the aim of reaching the same initial absorbance where possible. Subsequent 365 nm irradiations of (b) were performed for 60 s each.

(Figure 2a). Comparing the behavior under air and argon did not evidence any clear role of O_2 (see the SI, Figure S4). In contrast, a stable absorbance value was achieved following four cycles in the ClBenz:toluene system (Figure 3a), with the rate of the cascade effect increasing with the number of cycles. This may be attributed to the presence of a small amount of remnant $OF^{\bullet+}$ **TA0** along with solvent-based radicals that remain even after the cycloreversion of all CF **TA0**.[12] This is further supported by the increasing 365 nm irradiation time needed to reach the same amount of CF **TA0** for each cycle. At the end of each full ring opening after 254 nm irradiation, the amount of remaining $OF^{\bullet+}$ **TA0** or solvent-based radicals increases, triggering the cycloreversion of newly formed CF **TA0** at the start of the next cycle, that competes with photocyclization. Furthermore, the first cycle of Figure 3a shows a sigmoidal curve, suggesting delayed behavior for the cascade effect. This was also observed for several other halogenated solvents used (Figure 1). In a previous report using 9:1 chloroform:toluene, this behavior was not observed;[25] hence, it is expected that increasing the ratio of ClBenz to toluene should suppress this delayed effect.

The stability of CF **TA0** under several rounds of irradiation (60 s) at 365 nm was followed. In the chloroform:toluene system, a slight decrease in absorbance after four irradiation cycles was observed, indicating some detectable cycloreversion (Figure 2b). Alternatively, in the ClBenz:toluene system under the same conditions, absorbance increased after each irradiation, showing that no visible cycloreversion occurs on the same time scale (Figure 3b). Finally, 254 nm irradiation was performed on both solvent systems to observe their cascade behavior. The ClBenz:toluene system showed a slower CE fading, further supporting the increased stability of the CF **TA0** in this environment. We also conclude that under such conditions, irradiation at 254 nm is selective in triggering the cascade and provides suitable conditions for the reuse of our system. Initial assessments also demonstrated the sensitivity of **TA0** in ClBenz:toluene to X-ray triggered CE, showing its potential in X-ray detection (see the SI, Figure S5), with larger doses resulting in faster CE fading. These results also indicate

https://doi.org/10.1021/acsami.4c09023
ACS Appl. Mater. Interfaces 2024, 16, 57626−57635

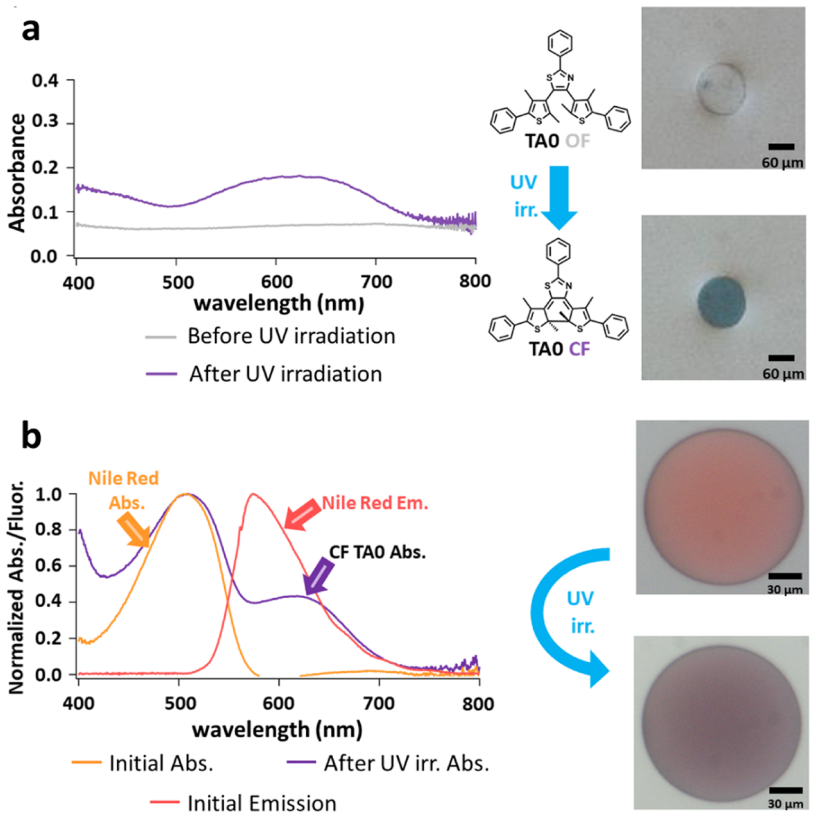

Figure 4. (a) Absorption spectra of a single microcapsule containing **TA0** ([TA0] = 0.5 mM) before (gray line; upper right image) and after (purple line; lower right image) UV irradiation at 365 nm. (b) Absorption/emission spectra of **TA0** + **NR** in a microcapsule with optical images before (yellow and orange lines, respectively; upper right image) and after (purple; lower right image) UV irradiation at 365 nm ([**TA0**] = 0.25 mM, [**NR**] = 0.05 mM).

the capability of repetitive X-ray detection by **TA0** in ClBenz:toluene.

3.2. Experiments in Microcapsules. *3.2.1. Preparation of Chromophoric Microcapsules.* During the fabrication process, it was observed that the precursor emulsion layer must be less dense than water to produce microcapsules that remain stable over a long time scale. Thus, this restricted the ratio of halogenated solvents that could be used to test the cascade effect as they generally have densities above 1 g/L. When looking at the two best chloroform replacements, the densities of a 1:1 mixture of DCM or ClBenz with toluene are 1.099 and 0.986 g/L, respectively.[49−51] ClBenz:toluene was thus selected as the solvent system, which is simultaneously compatible to CE fading and stable microcapsule formation. Indeed, ClBenz:toluene microcapsules proved stable for at least one month when stored in the refrigerator in a water suspension, confirming the temporal durability of the microcapsule shell.

Microcapsules containing only **TA0** in pure toluene were initially synthesized to confirm that photochromism could be detected within the biopolymer shell. A single microcapsule containing **TA0** ([**TA0**]= 0.5 mM) was observed under an optical microscope, and its absorption spectra before and after UV irradiation (365 nm) were measured using a spectrograph (Figure 4a). The appearance of an absorption band in the visible range and a visual change of the microcapsules from colorless to blue after irradiation demonstrate their photochromic properties.

3.2.2. Photoswitchable Fluorescent Microcapsules. The commercial fluorophore Nile Red (**NR**) was chosen because of the favorable spectral overlap between its emission band and the visible absorption band of CF **TA0** in both solution (see the SI, Figure S6) and in pure toluene microcapsules (Figure 4b), to allow efficient fluorescence quenching of **NR**.[52] Upon sequential irradiation in the UV (310−380 nm) and the visible range (540−580 nm), an absorption band in the visible range appeared and disappeared, indicative of the ring-closing isomerism of **TA0**. This was also accompanied by a decrease and increase of fluorescence intensity from **NR** (Figure 5), revealing that fluorescence quenching is correlated with OF/CF **TA0** isomerization.

To further explore the relationship between **TA0** concentration and fluorescence quenching, microcapsules were made with 0.2 mM **NR** and different **TA0** concentrations (1.0, 3.0, 10, and 15 mM), and three samples were tested for each concentration. Each system was subjected to at least 10 cycles of ring closing and opening to prove sufficient fatigue resistance (Figure 6a). During UV irradiation, the extent of fluorescence quenching increases with **TA0** concentration, with almost complete quenching observed at 10 and 15 mM. During visible light irradiation, the fluorescence recovered to a minimum value of 80% compared to initial fluorescence for all samples.

The remaining fluorescence in the OFF (CF) state markedly decreased in the microcapsules having higher **TA0** concentrations or smaller donor−acceptor distances (Figure 6b). Here, we also display the calculated ratio in % of the fluorescence intensity remaining based on the FRET equation and upon emission reabsorption from CF **TA0** (see the SI, Calculation of the Remaining Fluorescence under the

https://doi.org/10.1021/acsami.4c09023
ACS Appl. Mater. Interfaces 2024, 16, 57626−57635

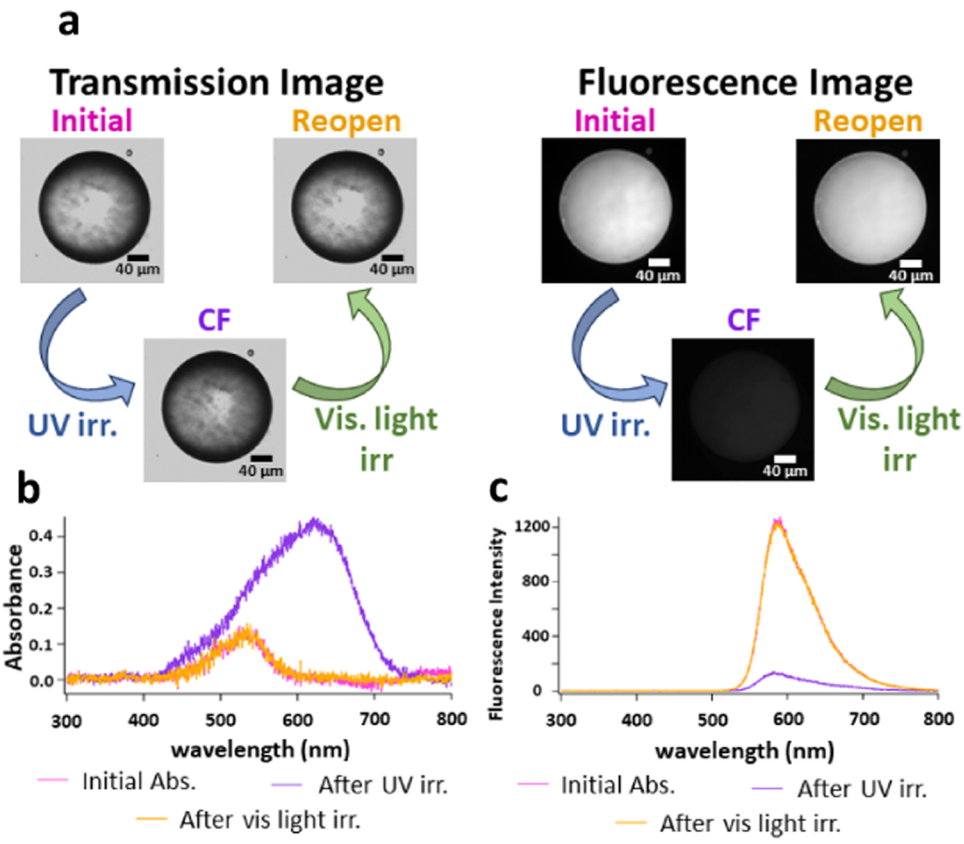

Figure 5. (a) Transmission (left) and fluorescence (right) images of each state of the microcapsule under ambient light and 450−495 nm excitation, respectively. (b) Absorption spectra (**TA0** and **NR**). (c) Fluorescence spectra (**NR**) of microcapsules after each step; [**TA0**] = 1 mM, [**NR**] = 0.2 mM.

Assumption of Emission Reabsorption and Table S2). The product of both calculations represents the process wherein the fluorophores not quenched by FRET could be quenched instead by reabsorption. At lower **TA0** concentrations (donor−acceptor distance >8 nm), around 80% of the fluorescence intensity remains, and the FRET has no impact on the fluorescence quenching. The microcapsules with 1 mM **TA0** showed more fluorescence quenching than the calculated results, which may stem from inhomogeneities within the microcapsules, forming localized areas with a high number of CF **TA0** molecules that quench **NR** more efficiently despite their lower concentrations. As the **TA0** concentration increases (donor−acceptor distances shorter than 5 nm), the contributions of FRET and emission reabsorption to quenching are similar. In this range, the calculated results roughly reproduce the observed fluorescence quenching. The minor discrepancy between the calculated and experimental values may also originate from the diverse shapes and sizes of the microcapsules, as fluorescence quenching experiments were conducted on single capsules. It should also be noted that both the experiment and calculation clearly denote the importance of **TA0** concentration higher than 10 mM to ensure fluorescence quenching over 90%. Considering the extinction coefficients of OF **TA0**, CF **TA0**, and **NR**, it is necessary to use a sufficiently short optical path length to achieve light penetration for photoinduced coloration and fading. In other words, no FRET quenching effect is possible for bulk solution experiments in a 1 cm cuvette of usual concentration (i.e., 1 mM or less). Efficient photochromic FRET quenching in this manner would require synthetic chemistry for bichromophore systems.[53] Thus, the present microcapsule system is advantageous for the simultaneous achievement of sufficiently short donor−acceptor distance and high optical penetration without complicated synthetic chemistry.

3.2.3. Cascade Effect in Microcapsules. The ability of the microcapsules to undergo a cascade effect following exposure to 254 nm irradiation was evaluated. Microcapsules of **TA0** ([**TA0**]= 5 mM) and **NR** ([**NR**] = 0.2 mM) in the 1:1 ClBenz:toluene system were fabricated and initially irradiated at 365 nm for 30 s to induce ring closing of **TA0**. This was followed by irradiation at 254 nm for 20 s to induce the cascade, and then, the system was kept in the dark. The change in NR fluorescence intensity together with the changes in **TA0** absorbance was measured for 1 h (Figure 7). The first 10 min showed a fast decay in the absorbance at 610 nm, followed by a more gradual decay. Furthermore, this absorbance decrease was accompanied by a mirror fluorescence recovery of **NR** at 575 nm. This is the first example of the cascade effect being observed in microcapsules and of fluorophores being used to track this phenomenon. We further observed repetitive UV-induced coloration and cascade fading cycles in a microcapsule of a larger size. Fluorescence photoswitching was also observed for four cycles, which will be reported elsewhere in relation to size effects.

4. CONCLUSIONS

An alternative to chloroform as an initiator for the chain-like oxidative cycloreversion reaction of terarylenes that allows switchability and microencapsulation has been investigated, and a microcapsule with fluorescence switching in conjunction

https://doi.org/10.1021/acsami.4c09023
ACS Appl. Mater. Interfaces 2024, 16, 57626−57635

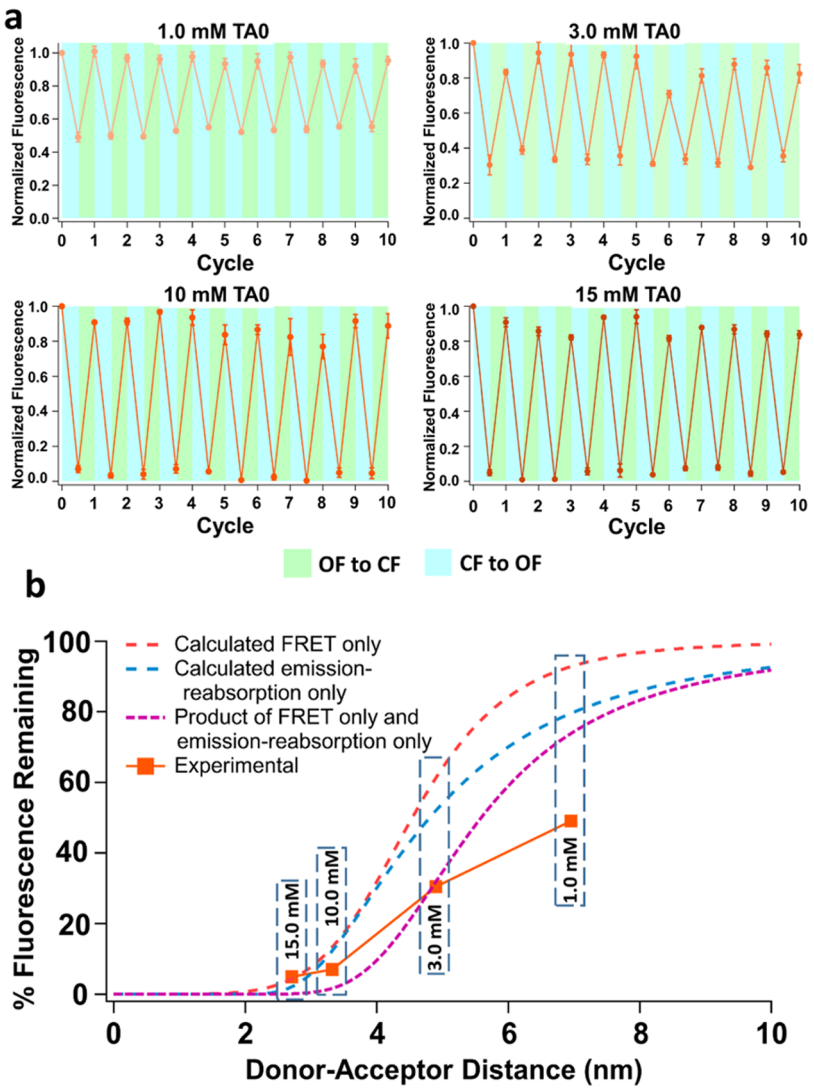

Figure 6. (a) Average fluorescence ON/OFF (OF to CF: 300−380 nm irradiation, 10 s; CF to OF: 540−580 nm irradiation, 10 s) cycles of three microcapsules composed of 0.2 mM **NR** and varying concentrations of **TA0** in toluene. Each of the three microcapsules was prepared from the same batch and measured individually. (b) Percentage of remaining fluorescence in the OFF state as a function of mean donor−acceptor distance. Experimentally observed data from Figure 6a are denoted by an orange marks and line. Calculated results based on the FRET equation and emission reabsorption equations are presented by red and blue lines, respectively. The products of both are presented as the purple line. Total **TA0** concentrations are indicated in the blue boxes and donor−acceptor distance calculations are based on CF **TA0** concentrations (see the SI, Choice of TA0 and NR Concentrations for Microcapsule Experiments and Table S1).

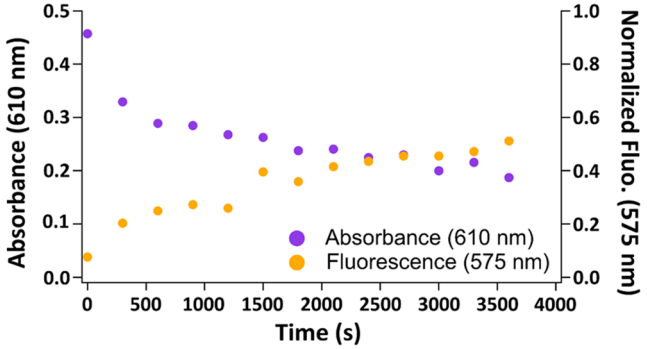

Figure 7. Time-dependent evolution of NR fluorescence (575 nm) and **TA0** absorbance (610 nm) after an initial 30 s of 254 nm irradiation.

with the cascade effect was demonstrated for the first time. A mixed solvent system containing equal volumes of chlorobenzene and toluene was found to induce a slower cascade effect but with better wavelength selectivity. In free solution, this system allows for both ring closing of the chosen terarylene derivative at 365 nm and UV-induced cycloreversion by the cascade effect at 254 nm without the need to add or remove the halogenated solvent, suggesting the possibility of reversible cascade-controlled fluorescence switching. When microencapsulated together with the fluorophore Nile Red, the photochrome enabled stable ON/OFF fluorescence switching via a combination of emission reabsorption and FRET processes in response to light irradiation. The system was durable for up to 10 cycles without decrease in the switching properties, and kinetic studies showed that the cascade effect was accompanied by the recovery of Nile Red emission, making it the first time that the two phenomena could be observed in a single system. This system offers an important

https://doi.org/10.1021/acsami.4c09023
ACS Appl. Mater. Interfaces 2024, 16, 57626−57635

step in the development of organic microcapsule detectors for high-energy radiation. Further work on this system may focus on improving the response time as well as X-ray sensitivity in microcapsules. Nonetheless, its improved properties and control make it well-suited for applications and could lead to the production of organic compound-based commercial devices.

■ ASSOCIATED CONTENT

Supporting Information

The Supporting Information is available free of charge at https://pubs.acs.org/doi/10.1021/acsami.4c09023.

Synthesis of **TA0** and microcapsules; experimental conditions for experiments in solution; effect of the DCM ratio on the cascade effect of **TA0**; absorption spectra of CF **TA0** and **NR** in solution; emission spectra of **NR** in solution; and quenching-related calculations for microcapsule experiments (PDF)

■ AUTHOR INFORMATION

Corresponding Authors

Tsuyoshi Kawai − *Graduate School of Science and Technology, Nara Institute of Science and Technology, NAIST, Ikoma, Nara 630-0192, Japan; Medilux Resaerch Center, Nara Institute of Science and Technology, NAIST, Ikoma, Nara 630-0192, Japan;* orcid.org/0000-0002-9566-3573; Email: tkawai@ms.naist.jp

Kazuma Yasuhara − *Graduate School of Science and Technology, Nara Institute of Science and Technology, NAIST, Ikoma, Nara 630-0192, Japan;* orcid.org/0000-0003-0701-6884; Email: yasuhara@ms.naist.jp

Authors

Magin Benedict Ferrer − *Graduate School of Science and Technology, Nara Institute of Science and Technology, NAIST, Ikoma, Nara 630-0192, Japan; Université Paris-Saclay, ENS Paris-Saclay, CNRS, PPSM, Gif-sur-Yvette 91190, France;* orcid.org/0000-0002-4725-5938

Daiyu Harada − *Graduate School of Science and Technology, Nara Institute of Science and Technology, NAIST, Ikoma, Nara 630-0192, Japan*

Colin J. Martin − *Graduate School of Science and Technology, Nara Institute of Science and Technology, NAIST, Ikoma, Nara 630-0192, Japan;* Present Address: C.J.M.: Laboratory for Chemistry and Life Science, Institute of Innovative Research, Tokyo Institute of Technology, Yokohama 226-8503, Japan

Rémi Métivier − *Université Paris-Saclay, ENS Paris-Saclay, CNRS, PPSM, Gif-sur-Yvette 91190, France*

Clémence Allain − *Université Paris-Saclay, ENS Paris-Saclay, CNRS, PPSM, Gif-sur-Yvette 91190, France*

Keitaro Nakatani − *Université Paris-Saclay, ENS Paris-Saclay, CNRS, PPSM, Gif-sur-Yvette 91190, France*

Marine Louis − *Graduate School of Science and Technology, Nara Institute of Science and Technology, NAIST, Ikoma, Nara 630-0192, Japan;* Present Address: M.L.: Department of Applied Chemistry, Graduate School of Engineering, Tokyo University of Agriculture and Technology, Nakamachi, Koganei-shi, Tokyo 184-8588, Japan; orcid.org/0000-0002-7298-8690

Noriaki Kawaguchi − *Graduate School of Science and Technology, Nara Institute of Science and Technology, NAIST, Ikoma, Nara 630-0192, Japan*

Takayuki Yanagida − *Graduate School of Science and Technology, Nara Institute of Science and Technology, NAIST, Ikoma, Nara 630-0192, Japan*

Complete contact information is available at: https://pubs.acs.org/10.1021/acsami.4c09023

Author Contributions

#M.B.F. and D.H. contributed equally to this paper. The manuscript was written through contributions of all authors. All authors have given approval to the final version of the manuscript.

Funding

IDEX Paris-Saclay IRP Synergetics JSPS KAKENHI

Notes

The authors declare no competing financial interest.

■ ACKNOWLEDGMENTS

This work is part of a project in collaboration with the Supramolecular and Macromolecular Photophysics and Photochemistry (PPSM) laboratory and the Laboratory of Photonic and Reactive Molecular Science in NAIST. This work is supported by the "ADI 2021" project funded by the IDEX Paris-Saclay, ANR-11-IDEX-0003-02. C.J.M. thanks the JSPS KAKENHI Grant-in-Aid for Early-Career Scientists 19K15312. T.K. thanks the JSPS KAKENHI, Grant-in-Aid for Scientific Research (B) JP22H02052 and for Transformative Research Area (A) JP23H04876, for the financial support. This collaboration is in the framework of CNRS IRP Nanosynergetics. T.K. also acknowledges the support of ARIM-Japan/NAIST (#JPMXP1224NR5023).

■ ABBREVIATIONS

CE –cascade effect; DAE –diarylethene; TA –terarylene; $TBPA^{\bullet+}$ -, CF –closed form; OF –open form; FRET –Förster resonance energy transfer; PSS –photostationary state; DCM –dichloromethane; 1-ClBut –1-chlorobutane; 1-BrProp –1-bromopropane; TeClEt –tetrachloroethane; ClBenz –chlorobenzene; BrBenz –bromobenzene; *o*-DiClBenz –o-dichlorobenzene; **NR** –Nile Red

■ REFERENCES

(1) Kume, H.; Koyama, K.; Nakatsugawa, K.; Suzuki, S.; Fatlowitz, D. Ultrafast Microchannel Plate Photomultipliers. *Appl. Opt.* **1988**, *27* (6), No. 1170.

(2) Otte, A. N.; Garcia, D.; Nguyen, T.; Purushotham, D. Characterization of Three High Efficiency and Blue Sensitive Silicon Photomultipliers. *Nucl. Instrum. Methods Phys. Res., Sect. A* **2017**, *846*, 106−125.

(3) Nagai, A.; Alispach, C.; Barbano, A.; Coco, V.; Della Volpe, D.; Heller, M.; Montaruli, T.; Ekoume, S. N.; Troyano-Pujadas, I.; Renier, Y. Characterization of a Large Area Silicon Photomultiplier. *Nucl. Instrum. Methods Phys. Res., Sect. A* **2019**, *948*, No. 162796.

(4) Gallina, G.; Giampa, P.; Retière, F.; Kroeger, J.; Zhang, G.; Ward, M.; Margetak, P.; Li, G.; Tsang, T.; Doria, L.; Al Kharusi, S.; Alfaris, M.; Anton, G.; Arnquist, I. J.; Badhrees, I.; Barbeau, P. S.; Beck, D.; Belov, V.; Bhatta, T.; Blatchford, J.; Brodsky, J. P.; Brown, E.; Brunner, T.; Cao, G. F.; Cao, L.; Cen, W. R.; Chambers, C.; Charlebois, S. A.; Chiu, M.; Cleveland, B.; Coon, M.; Craycraft, A.;

Dalmasson, J.; Daniels, T.; Darroch, L.; Daugherty, S. J.; De St Croix, A.; Der Mesrobian-Kabakian, A.; DeVoe, R.; Dilling, J.; Ding, Y. Y.; Dolinski, M. J.; Dragone, A.; Echevers, J.; Elbeltagi, M.; Fabris, L.; Fairbank, D.; Fairbank, W.; Farine, J.; Feyzbakhsh, S.; Fontaine, R.; Gautam, P.; Giacomini, G.; Gornea, R.; Gratta, G.; Hansen, E. V.; Heffner, M.; Hoppe, E. W.; Hößl, J.; House, A.; Hughes, M.; Ito, Y.; Iverson, A.; Jamil, A.; Jewell, M. J.; Jiang, X. S.; Karelin, A.; Kaufman, L. J.; Kodroff, D.; Koffas, T.; Krücken, R.; Kuchenkov, A.; Kumar, K. S.; Lan, Y.; Larson, A.; Lenardo, B. G.; Leonard, D. S.; Li, S.; Li, Z.; Licciardi, C.; Lin, Y. H.; Lv, P.; MacLellan, R.; McElroy, T.; Medina-Peregrina, M.; Michel, T.; Mong, B.; Moore, D. C.; Murray, K.; Nakarmi, P.; Newby, R. J.; Ning, Z.; Njoya, O.; Nolet, F.; Nusair, O.; Odgers, K.; Odian, A.; Oriunno, M.; Orrell, J. L.; Ortega, G. S.; Ostrovskiy, I.; Overman, C. T.; Parent, S.; Piepke, A.; Pocar, A.; Pratte, J.-F.; Qiu, D.; Radeka, V.; Raguzin, E.; Rescia, S.; Richman, M.; Robinson, A.; Rossignol, T.; Rowson, P. C.; Roy, N.; Saldanha, R.; Sangiorgio, S.; Skarpaas, K.; Soma, A. K.; St-Hilaire, G.; Stekhanov, V.; Stiegler, T.; Sun, X. L.; Tarka, M.; Todd, J.; Tolba, T.; Totev, T. I.; Tsang, R.; Vachon, F.; Veeraraghavan, V.; Visser, G.; Vuilleumier, J.-L.; Wagenpfeil, M.; Walent, M.; Wang, Q.; Watkins, J.; Weber, M.; Wei, W.; Wen, L. J.; Wichoski, U.; Wu, S. X.; Wu, W. H.; Wu, X.; Xia, Q.; Yang, H.; Yang, L.; Yen, Y.-R.; Zeldovich, O.; Zhao, J.; Zhou, Y.; Ziegler, T. Characterization of the Hamamatsu VUV4MPPCs for nEXO. *Nucl. Instrum. Methods Phys. Res., Sect. A* **2019**, *940*, 371−379.

(5) Ando, H.; Kanbe, H.; Ito, M.; Kaneda, T. Tunneling Current in InGaAs and Optimum Design for InGaAs/InP Avalanche Photodiode. *Jpn. J. Appl. Phys.* **1980**, *19* (6), No. L277.

(6) Capasso, F.; Cho, A. Y.; Foy, P. W. Low-Dark-Current Low-Voltage 1.3−1.6 Mm Avalanche Photodiode with High-Low Electric Field Profile and Separate Absorption and Multiplication Regions by Molecular Beam Epitaxy. *Electron. Lett.* **1984**, *20* (15), 635−637.

(7) Irie, M. Diarylethenes for Memories and Switches. *Chem. Rev.* **2000**, *100* (5), 1685−1716.

(8) Ishibashi, Y.; Okuno, K.; Ota, C.; Umesato, T.; Katayama, T.; Murakami, M.; Kobatake, S.; Irie, M.; Miyasaka, H. Multiphoton-Gated Cycloreversion Reactions of Photochromic Diarylethene Derivatives with Low Reaction Yields upon One-Photon Visible Excitation. *Photochem. Photobiol. Sci.* **2010**, *9* (2), No. 172.

(9) Irie, M.; Fukaminato, T.; Matsuda, K.; Kobatake, S. Photochromism of Diarylethene Molecules and Crystals: Memories, Switches, and Actuators. *Chem. Rev.* **2014**, *114* (24), 12174−12277.

(10) Rybalkin, V. P.; Pluzhnikova, S. Yu.; Popova, L. L.; Revinskii, Y. V.; Tikhomirova, K. S.; Komissarova, O. A.; Dubonosov, A. D.; Bren, V. A.; Minkin, V. I. A Novel Approach to Fluorescent Photochromic Fulgides. *Mendeleev Commun.* **2016**, *26* (1), 21−23.

(11) Nakashima, T.; Kajiki, Y.; Fukumoto, S.; Taguchi, M.; Nagao, S.; Hirota, S.; Kawai, T. Efficient Oxidative Cycloreversion Reaction of Photochromic Dithiazolylthiazole. *J. Am. Chem. Soc.* **2012**, *134* (48), 19877−19883.

(12) Calupitan, J. P.; Nakashima, T.; Hashimoto, Y.; Kawai, T. Fast and Efficient Oxidative Cycloreversion Reaction of a π-Extended Photochromic Terarylene. *Chem. - Eur. J.* **2016**, *22* (29), 10002−10008.

(13) Staykov, A.; Areephong, J.; Browne, W. R.; Feringa, B. L.; Yoshizawa, K. Electrochemical and Photochemical Cyclization and Cycloreversion of Diarylethenes and Diarylethene-Capped Sexithiophene Wires. *ACS Nano* **2011**, *5* (2), 1165−1178.

(14) Léaustic, A.; Anxolabéhère-Mallart, E.; Maurel, F.; Midelton, S.; Guillot, R.; Métivier, R.; Nakatani, K.; Yu, P. Photochromic and Reductive Electrochemical Switching of a Dithiazolylethene with Large Redox Modulation. *Chem. - Eur. J.* **2011**, *17* (7), 2246−2255.

(15) Nakashima, T.; Atsumi, K.; Kawai, S.; Nakagawa, T.; Hasegawa, Y.; Kawai, T. Photochromism of Thiazole-Containing Triangle Terarylenes. *Eur. J. Org. Chem.* **2007**, *2007* (19), 3212−3218.

(16) Kutsunugi, Y.; Kawai, S.; Nakashima, T.; Kawai, T. Photochromic Properties of Terarylene Derivatives Having a π-Conjugation Unit on Central Aromatic Ring. *New J. Chem.* **2009**, *33* (6), No. 1368.

(17) Peters, A.; McDonald, R.; Branda, N. R. Regulating π-Conjugated Pathways Using a Photochromic 1,2-Dithienylcyclopentene. *Chem. Commun.* **2002**, No. 19, 2274−2275.

(18) Martin, C. J.; Goto, Y.; Asato, R.; Rapenne, G.; Kawai, T. Investigations into Oxidation Induced Ring Opening of Terarylenes Containing π-Extended Thieno[*b*]Thiophene Units. *New J. Chem.* **2023**, *47* (6), 2832−2839.

(19) Gorodetsky, B.; Branda, N. R. Bidirectional Ring-Opening and Ring-Closing of Cationic 1,2-Dithienylcyclopentene Molecular Switches Triggered with Light or Electricity. *Adv. Funct. Mater.* **2007**, *17* (5), 786−796.

(20) Gorodetsky, B.; Samachetty, H. D.; Donkers, R. L.; Workentin, M. S.; Branda, N. R. Reductive Electrochemical Cyclization of a Photochromic 1,2-Dithienylcyclopentene Dication. *Angew. Chem., Int. Ed.* **2004**, *43* (21), 2812−2815.

(21) Koshido, T.; Kawai, T.; Yoshino, K. Optical and Electrochemical Properties of Cis-1,2-Dicyano-1,2-Bis(2,4,5-Trimethyl-3-Thienyl)Ethene. *J. Phys. Chem. A* **1995**, *99* (16), 6110−6114.

(22) Moriyama, Y.; Matsuda, K.; Tanifuji, N.; Irie, S.; Irie, M. Electrochemical Cyclization/Cycloreversion Reactions of Diarylethenes. *Org. Lett.* **2005**, *7* (15), 3315−3318.

(23) Browne, W. R.; Kudernac, T.; Katsonis, N.; Areephong, J.; Hjelm, J.; Feringa, B. L. Electro- and Photochemical Switching of Dithienylethene Self-Assembled Monolayers on Gold Electrodes. *J. Phys. Chem. C* **2008**, *112* (4), 1183−1190.

(24) Guirado, G.; Coudret, C.; Launay, J.-P. Electrochemical Remote Control for Dithienylethene-Ferrocene Switches. *J. Phys. Chem. C* **2007**, *111* (6), 2770−2776.

(25) Asato, R.; Martin, C. J.; Calupitan, J. P.; Mizutsu, R.; Nakashima, T.; Okada, G.; Kawaguchi, N.; Yanagida, T.; Kawai, T. Photosynergetic Amplification of Radiation Input: From Efficient UV Induced Cycloreversion to Sensitive X-Ray Detection. *Chem. Sci.* **2020**, *11* (9), 2504−2510.

(26) Kamiya, K.; Ozasa, K.; Akiba, S.; Niwa, O.; Kodama, K.; Takamura, N.; Zaharieva, E. K.; Kimura, Y.; Wakeford, R. Long-Term Effects of Radiation Exposure on Health. *Lancet* **2015**, *386* (9992), 469−478.

(27) Nondestructive Evaluation NDE Engineering: Radiation Safety. https://www.nde-ed.org/NDEEngineering/RadiationSafety/radiation_safety_equipment/film_badges.xhtml (accessed February 28, 2024).

(28) Chand, S.; Mehra, R.; Chopra, V. Recent Developments in Phosphate Materials for Their Thermoluminescence Dosimeter (TLD) Applications. *Luminescence* **2021**, *36* (8), 1808−1817.

(29) Yukihara, E. G.; McKeever, S. W. S.; Akselrod, M. S. State of Art: Optically Stimulated Luminescence Dosimetry − Frontiers of Future Research. *Radiat. Meas.* **2014**, *71*, 15−24.

(30) Yamamoto, T.; Maki, D.; Sato, F.; Miyamoto, Y.; Nanto, H.; Iida, T. The Recent Investigations of Radiophotoluminescence and Its Application. *Radiat. Meas.* **2011**, *46* (12), 1554−1559.

(31) Vanhavere, F.; Van Hoey, O. Advances in Personal Dosimetry towards Real-Time Dosimetry. *Radiat. Meas.* **2022**, *158*, No. 106862.

(32) Pavelic, L.; Lackovic, I.; Mihic, M. S.; Prlic, I. A Technology Overview of Active Ionizing Radiation Dosemeters for Photon Fields. *Radiat. Prot. Dosim.* **2020**, *188* (3), 361−371.

(33) Mittal, A.; Verma, S.; Natanasabapathi, G.; Kumar, P.; Verma, A. K. Diacetylene-Based Colorimetric Radiation Sensors for the Detection and Measurement of γ Radiation during Blood Irradiation. *ACS Omega* **2021**, *6* (14), 9482−9491.

(34) Kinashi, K.; Iwata, T.; Tsuchida, H.; Sakai, W.; Tsutsumi, N. Composite Resin Dosimeters: A New Concept and Design for a Fibrous Color Dosimeter. *ACS Appl. Mater. Interfaces* **2018**, *10* (14), 11926−11932.

(35) Kinashi, K.; Miyamae, Y.; Nakamura, R.; Sakai, W.; Tsutsumi, N.; Yamane, H.; Hatsukano, G.; Ozaki, M.; Jimbo, K.; Okabe, T. A Spiropyran-Based X-Ray Sensitive Fiber. *Chem. Commun.* **2015**, *51* (56), 11170−11173.

https://doi.org/10.1021/acsami.4c09023
ACS Appl. Mater. Interfaces 2024, 16, 57626−57635

(36) Irie, S.; Irie, M. Ultrahigh Sensitive Color Dosimeters Composed of Photochromic Diarylethenes and Fluorescent Metal Complexes. *Chem. Lett.* **2006**, *35* (12), 1434−1435.
(37) Yamaguchi, T.; Irie, M. Ultrahigh-sensitive fluorescence dosimeters that use turn-on mode fluorescent diarylethenes. *Tetrahedron Lett.* **2020**, *61* (35), No. 152232.
(38) Butterfield, J. L.; Penoncello, G. P.; Dikshit, K.; Bruns, C. J. Photochromic Intradermal Smart Tattoo Based on Diarylethene-Doped Polystyrene Nanoparticles for Personal γ-Ray Dosimetry. *ACS Appl. Nano Mater.* **2022**, *5* (10), 13840−13844.
(39) Han, J.-M.; Xu, M.; Wang, B.; Wu, N.; Yang, X.; Yang, H.; Salter, B. J.; Zang, L. Low Dose Detection of γ Radiation via Solvent Assisted Fluorescence Quenching. *J. Am. Chem. Soc.* **2014**, *136* (13), 5090−5096.
(40) Bansode, S. S.; Banarjee, S. K.; Gaikwad, D. D.; Jadhav, S. L.; Thorat, R. M. Microencapsulation: A Review. *Int. J. Pharm. Sci. Rev. Res.* **2010**, *1* (2), 38−43.
(41) Yan, C.; Kim, S.-R.; Ruiz, D. R.; Farmer, J. R. Microencapsulation for Food Applications: A Review. *ACS Appl. Bio Mater.* **2022**, *5* (12), 5497−5512.
(42) Li, C.; Gong, W.-L.; Hu, Z.; Aldred, M. P.; Zhang, G.-F.; Chen, T.; Huang, Z.-L.; Zhu, M.-Q. Photoswitchable Aggregation-Induced Emission of a Dithienylethene−Tetraphenylethene Conjugate for Optical Memory and Super-Resolution Imaging. *RSC Adv.* **2013**, *3* (23), No. 8967.
(43) An, B.-K.; Kwon, S.-K.; Jung, S.-D.; Park, S. Y. Enhanced Emission and Its Switching in Fluorescent Organic Nanoparticles. *J. Am. Chem. Soc.* **2002**, *124* (48), 14410−14415.
(44) Leong, J.-Y.; Tey, B.-T.; Tan, C.-P.; Chan, E.-S. Nozzleless Fabrication of Oil-Core Biopolymeric Microcapsules by the Interfacial Gelation of Pickering Emulsion Templates. *ACS Appl. Mater. Interfaces* **2015**, *7* (30), 16169−16176.
(45) Irie, M.; Sayo, K. Solvent Effects on the Photochromic Reactions of Diarylethene Derivatives. *J. Phys. Chem. A* **1992**, *96* (19), 7671−7674.
(46) Tian, W.; Tian, J. An Insight into the Solvent Effect on Photo-, Solvato-Chromism of Spiropyran through the Perspective of Intermolecular Interactions. *Dyes Pigm.* **2014**, *105*, 66−74.
(47) El-Hendawy, M. M.; Fayed, T. A.; Awad, M. K.; English, N. J.; Etaiw, S. E. H.; Zaki, A. B. Photophysics, Photochemistry and Thermal Stability of Diarylethene-Containing Benzothiazolium Species. *J. Photochem. Photobiol., A* **2015**, *301*, 20−31.
(48) Liu, S.; Huang, W.; Yang, J.; Xiong, Y.; Huang, Z.; Wang, J.; Cai, T.; Dang, Z.; Yang, C. Formation of Environmentally Persistent Free Radicals on Microplastics under UV Irradiations. *J. Hazard. Mater.* **2023**, *453*, No. 131277.
(49) Dichlorométhane | Sigma-Aldrich. http://www.sigmaaldrich.com/ (accessed September 19, 2023).
(50) Chlorobenzene anhydrous, 99.8% | Sigma-Aldrich. http://www.sigmaaldrich.com/ (accessed September 19, 2023).
(51) Toluene Density. https://echa.europa.eu/registration-dossier/-/registered-dossier/15538/4/5 (accessed September 19, 2023).
(52) Wu, L.; Huang, C.; Emery, B. P.; Sedgwick, A. C.; Bull, S. D.; He, X.-P.; Tian, H.; Yoon, J.; Sessler, J. L.; James, T. D. Förster Resonance Energy Transfer (FRET)-Based Small-Molecule Sensors and Imaging Agents. *Chem. Soc. Rev.* **2020**, *49* (15), 5110−5139.
(53) Irie, M.; Fukaminato, T.; Sasaki, T.; Tamai, N.; Kawai, T. A digital fluorescent molecular photoswitch. *Nature* **2002**, *420*, 759−760.

https://doi.org/10.1021/acsami.4c09023
ACS Appl. Mater. Interfaces 2024, 16, 57626−57635